

**Article citation info:**

Nycz D B. Effect of the B-type guiderail joints of a road barrier on the TB11 and TB32 virtual crash tests. The Archives of Automotive Engineering – Archiwum Motoryzacji. 2016; 71(1): 73-85, <http://dx.doi.org/10.14669/AM.VOL71.ART4>

# EFFECT OF THE B-TYPE GUIDERAIL JOINTS OF A ROAD BARRIER ON THE TB11 AND TB32 VIRTUAL CRASH TESTS

**DANIEL B. NYCZ<sup>1</sup>**

Jan Grodek State Vocational Academy in Sanok

## Summary

The work presents the effect of the B-type guiderail joints of the SP-05/2 barrier, of the N2-W4-A class, on the course of the TB11 and TB32 virtual crash tests. The guiderail was modelled as a continuous beam (without joints) and as a system consisting of 4 m long segments connected by beam elements reflecting screw joints. The TB11 test concerns a passenger car with a mass of 900 kg, impacting onto barrier with a velocity of 100 km/h, at an angle of 20°. The TB32 test concerns a passenger car with a mass of 1500 kg, onto barrier with a velocity of 110 km/h, at an angle of 20°. The numerical calculations were done using the LS-Dyna finite element code, with the use of Geo Metro and Dodge Neon car models taken from the National Crash Analysis Center (NCAC) public library. The car models were modified to the relevant extent. The results of the virtual crash tests were analyzed with respect to the parameters and acceptance criteria of crash tests, as required by PN-EN 1317-1:2010 and PN-EN 1317-2:2010 standards. Taking the guiderail segment joints into consideration enables checking whether the guiderail will maintain continuity during a crash test. Modelling crash tests with guiderails modelled as a continuous beams results in decreasing nearly all crash parameters, and in case of the TB11 test – in smoother repulse of the car.

**Keywords:** protective road barrier, guiderail segment joints, virtual crash tests, numerical modelling

## 1. Introduction

Virtual crash tests of road restraint systems are a subject of many studies. Steel protective barriers have been subjected to virtual and experimental crash tests, e.g. in the studies [1, 2, 5, 12, 13]. They present various numerical models of systems consisting of a vehicle and a restraint system. The study [5] covers a comparison of results of the TB11 and TB32

<sup>1</sup> Jan Grodek State Vocational Academy in Sanok, Technical Institute, ul. Reymonta 6, 38-500 Sanok, Poland, e-mail: [daniel.nycz@interia.pl](mailto:daniel.nycz@interia.pl)

crash tests, both experimental and virtual, in reference to eight assorted road barriers. The authors point out the sensitivity of a numerical model to changes of certain parameters of the model. They also pay attention to random features of the vehicle/barrier systems (material properties, crash test criteria tolerances, measurement errors). The authors mention three typical forms of barrier damage: plastic deformation of the guiderail, bending of posts and plastic hinge in the restraint section in the subsoil, breaking of the joint between a guiderail and a post.

The study [12] concerned an analysis of a road barrier with an A-type guiderail, employing easily-deformable spacer elements connecting the guiderail with the posts. In the modelling, it was assumed that the guiderail is a continuous beam. Numerical results of the TB11 test were compared with the experimental results (the comparison only included the ASI index and the working width  $W$ ).

Modelling and simulations of the TB11 and TB42 crash tests for a system of the H1 containment level were performed in the study [2]. It investigated the effect of four structural changes in the road barrier: 1) introduction of a tension belt, 2) introduction of a roll guide, 3) introduction of a rope in the top part of the guiderail, 4) introduction of a rope in the bottom part of the guiderail. Virtual crash tests were compared with the experimental tests. Vehicle models were taken from the NCAC public library [18] and several modifications were introduced. The guiderail was modelled as a continuous beam (without joints). Other screw joints of the barrier were reflected using beam elements or the SpotWeld type [6, 7]. The subsoil was modelled using elastic-damping elements.

Numerical modelling and simulations of crash tests required for the H1 containment level were performed in the study [13]. Calculations were performed in the LS-DYNA system. Vehicle numerical models were taken from the NCAC library [18]. Modifications were introduced into the models. Parts of the barrier were modelled using fully integrable shell elements with five integration points across the thickness in the impact zone, as well as Belytschko-Tsay shell elements with three integration points across the thickness – outside this zone. The guiderail/post screw joints were modelled using linear Hughes-Liu beam elements or SpotWeld constraints [6, 7]. The parameters of the joints were determined using an experimental numerical method based on the tensile test of joints. The subsoil was modelled using elastic viscoplastic constraints with characteristics dependent on the immersion depth of a post in the subsoil, as determined by the numerical-experimental method.

The simulation possibilities of road crash tests in the LS-DYNA system were presented in the study [1]. The subject of the study is a G4(1S) barrier with a W-type guiderail and over-rigid posts of the W150×13 type. In the vehicle impact zone, the guiderail and posts were modelled using shell elements in the Belytschko-Tsay formulation, with three integration points across the thickness. M32 screw joints were modelled in the simplified way. The subsoil was modelled using orthogonal elastic constraints up to the depth of 1 m. Outside the impact zone, only the longitudinal flexibility of the barrier was taken into consideration using elastic constraints. A model of a vehicle with a mass of 2000 kg was taken from the NCAC library [18] and appropriately modified. The simulation results were compared with a negative result of the experimental tests. The simulations were used to redesign the barrier in order to meet the acceptance criteria for crash tests.

The goal of the present study is to compare the effect of joints of a guiderail of the SP-05/2 system on the results of the TB11 and TB32 virtual crash tests. The guiderail was modelled as a continuous beam – without screw joints (codes: TB11\_C, TB32\_C), and as 4 m segments connected with beam elements reflecting screw joints (codes: TB11\_S, TB32\_S). The parameters and criteria of road crash tests, as required by the standards [14, 15], were analyzed.

## 2. The examined system and the analyzed crash tests

The subject of the study is a SP-05/2 extreme outer road barrier of the N2-W4-A class. The manufacturer of the system is the Stalprodukt S.A. company with principal office in Bochnia [16, 17]. The system can also be used on median strips (two parallel barriers).

The barrier consists of B-type guiderail sections with a total length of 4.30 m (effective length: 4.00 m), Sigma posts with a length of 1.9 m, as well as trapezoidal brackets and rectangular pads. All barrier elements are made of S235JR structural steel and subject to the process of hot-dip galvanizing. M16 bolts of the 4.6 class have been used as joints [16, 17].

The condition of approval of the N2-W4-A class road barrier for use is fulfillment of the conditions of standards [14, 15] in reference to the TB11 and TB32 crash tests. The TB11 test concerns a passenger car with a mass of 900 kg, impacting the barrier with a velocity of 100 km/h at an angle of 20°. The TB32 test concerns a passenger car with a mass of 1500 kg, impacting the barrier with a velocity of 110 km/h at an angle of 20°.

According to the product card [17], the SP-05/2 system meets the conditions of standards [14, 15] for the TB11 and TB32 crash tests. The manufacturer has given certain results of these tests: ASI = 0.8, THIV = 23.0 km/h, VCDI = RF0001000,  $W_m = 1.1$  m.

## 3. Crash test parameters

During crash tests, both a restraint system (in accordance with its performance class) and a vehicle should meet the requirements concerning: impact severity, deformation of the restraint system, behaviour of the restraining system, and behaviour of the vehicle under examination.

The ASI parameter (acceleration severity index) is a value describing the severity of motion during a collision with a restraining system to a person present near the point of measurement. It is calculated as a maximum value from the function [14, 15]:

$$ASI(t) = \sqrt{\left(\frac{\bar{a}_x(t)}{\bar{a}_x}\right)^2 + \left(\frac{\bar{a}_y(t)}{\bar{a}_y}\right)^2 + \left(\frac{\bar{a}_z(t)}{\bar{a}_z}\right)^2} \quad (1)$$

where:

$$\bar{a}_j(t) = \frac{1}{\delta} \int_z^{z+\delta} a_j(t) dt, \quad j=x,y,z \quad (2)$$

and  $\hat{a}_x, \hat{a}_y, \hat{a}_z$  – limit values of acceleration components in the directions  $x, y, z$  (in Europe, respectively, 12 g, 9 g, and 10 g);  $a_x(t), a_y(t), a_z(t)$  – acceleration components of the vehicle's centre of gravity;  $\bar{a}_x(t), \bar{a}_y(t), \bar{a}_z(t)$  – acceleration components of the vehicle's centre of gravity, passed through a Butterworth four-pole zero-phase digital filter, low-pass, cut-off frequency of 13 Hz (acceleration component values averaged over a moving time interval of  $\delta = 50$  ms);  $\delta = 50$  ms – moving time interval.

Impact severity levels assume the following values: level A:  $ASI \leq 1.0$ ; level B:  $ASI \leq 1.4$ ; level C:  $ASI \leq 1.9$  [14, 15].

The THIV parameter (theoretical head impact velocity), similarly as ASI, is used to assess the impact severity, in relation to persons in a vehicle, during a collision with a restraint system [14, 15]. It is assumed that a person inside a vehicle is an object (theoretical head) moving freely in such way that during a change of direction of motion of a vehicle (impact on the restraint system), the head continues moving straight-linearly and independently from the vehicle, until the moment of impact on an internal surface of the vehicle (a wall of a theoretical cabin). The value of velocity of the theoretical head impact on the moving theoretical cabin of the vehicle is the THIV parameter. The algorithm of determination of the THIV parameter can be found in the studies [11, 19]. For the impact severity levels A, B, C, the THIV value meets the condition of  $THIV \leq 33$  km/h [14, 15].

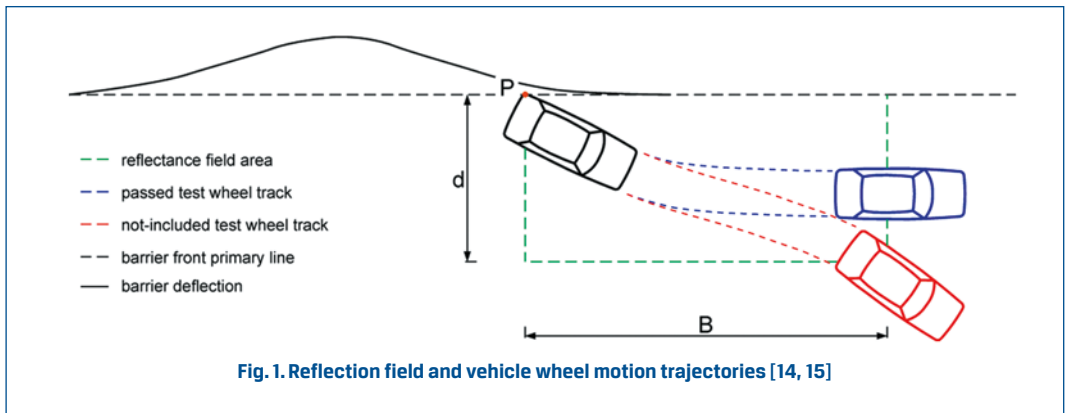
The vehicle cabin deformation index (VCDI) defines the normalized deformation of the interior of a vehicle. Expression of the VCDI parameter in the form of XYabcdefg covers both the location and extent of the vehicle cabin damage, where XY is the place of deformation of the vehicle cabin, and abcdefg are indices defining the percentage decrease of the seven internal dimensions of the vehicle cabin [14, 15].

The working width  $W_m$  is the maximum transversal distance between any part of the non-deformed barrier from the traffic side and the maximum dynamic position of any part of this barrier [14, 15].

After an impact, a passenger car with a length  $L$  [m] and width  $S$  [m] should deflect from the protective barrier in such way that the wheel track should not cross the line parallel to the original barrier line from the traffic side at the distance of

$$d = 2.2 + S + 0.16 L \quad (3)$$

within the distance limits  $B = 10.0$  m from the point P (point of the closest bottom edge of the protective barrier), in which the track of the last wheel of the vehicle crosses the barrier front line again on the traffic side after the initial impact (Fig. 1) [14, 15]. For the Geo Metro car (TB11 test), the result is  $d = 4.38$  m, and for the Dodge Neon car (TB32 test), it is  $d = 4.53$  m.



#### 4. Numeric models of the systems under analysis

The TB11 and TB32 virtual crash tests involved the use of the Geo Metro and Dodge Neon vehicle models developed by the NCAC [18]. The Geo Metro model includes above 33 000 finite elements (above 35 000 nodes). The Dodge Neon model includes above 279 000 finite elements (above 283 000 nodes). Initial crash tests (including central impact and impact of the vehicle at an angle of 20° on a rigid wall) showed a necessity to introduce many modifications and amendments into the vehicle model, including change of the model describing the work of tyres, correction of the suspension model, introduction of dynamic relaxation (gravity) before starting the process of vehicle/barrier collision, correction of the contact model options and control cards.

Sections of the SP-05/2 barrier with a length of 60 m were meshed using 4-node finite shell elements in the Belytschko-Tsay formulation, with integration reduced in the element plane (ELFORM\_2 formulation according to [6, 7]) and 5 integration points through the thickness.

The subsoil in which the steel SIGMA posts of the SP-05/2 barrier are embedded was reflected by cylinders with a radius of 1.00 m and height of 1.30 m. They were meshed with solid elements with the HEX8 and PENTA6 topology, with assigned ELFORM\_1 formulation (solid elements with permanent integration) [6, 7].

Elements made of S235JR structural steel (the SP-05/2 system) were described using an elasto-plastic model with isotropic hardening, taking into consideration the damage criterion based on the \*MAT\_024\_PIECEWISE\_LINEAR\_PLASTICITY effective plastic deformation [6, 7]. Material constants were taken from the product quality certificate of the Stalprodukt company [9-11]. The subsoil was described using the \*MAT\_005\_SOIL\_AND\_FOAM [6, 7] material model. It is a simple model used to describe the behaviour of foams and subsoil in case when their material constants are not fully defined. The material constants of the subsoil were taken from the NCAC site [18].

A crucial factor impacting the functionality of protective barriers is screw joints. In the system SP-05/2, there are screw joints between guiderails as well as between guiderails and SIGMA posts.

The studies [4, 11] show that the main and desired damage mechanism of screw joints between posts and guiderails is shear of a screw joint. Screw joints in these nodes have been modelled using \*CONSTRAINED\_GENERALIZED\_WELD\_SPOT [6, 7], with appropriate capacities resulting from the strength class of screws [17].

In many works, such as [2, 3, 12], a guiderail is treated as a continuous beam, omitting the screw joints between segments. The present study investigated the effect of these joints on the TB11 and TB32 virtual crash tests of the SP-05/2 barrier, modelling a guiderail as a continuous beam and as a beam consisting of screw-joined segments (Fig. 2).

For screw joints of guiderails, a method of determination of substitute rigidity characteristics has been developed [8-11]. The method is as follows: 1) determination of an experimental elasto-plastic characteristic of a single screw joint of guiderail segments, subjected to a test of tension with shear (cut out of a full 6-screw joint); 2) 3D modelling of a single screw joint in order to determine the options/parameters of modelling and simulation, leading to the numeric result being consistent with the experimental result; 3) 2D modelling (substitute model) of a single screw joint of guiderail segments using a beam element reflecting the rigidity characteristic of the joint; 4) 3D modelling of tension with shear of a full screw joint of guiderail segments using the determined options/parameters of modelling and simulation in order to determine the rigidity characteristic; 5) 2D modelling (substitute model) of a full screw joint of guiderail segments [8-11].

The screw joints of guiderail segments were represented as beam elements with assigned rigidity parameters determined on the basis of the method above (material model: \*MAT\_68\_NONLINEAR\_PLASTIC\_DISCRETE\_BEAM [6, 7]).

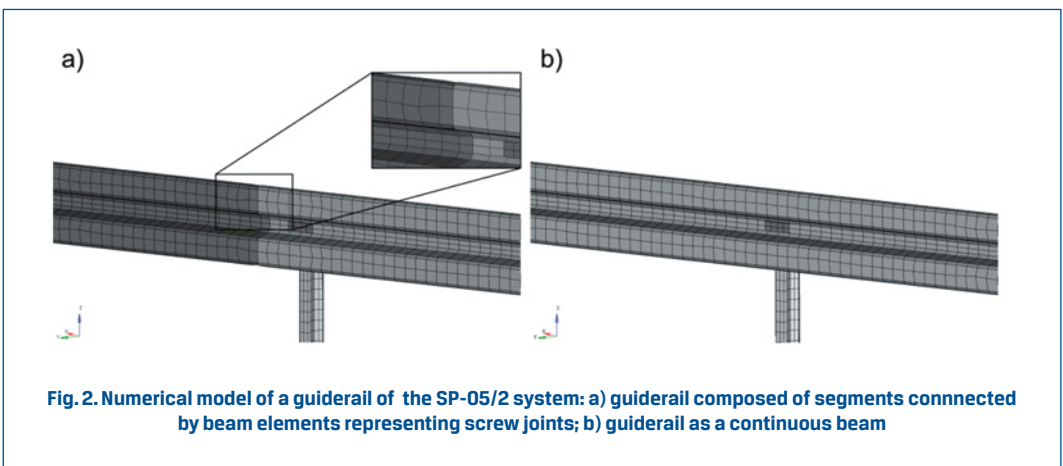


**Fig. 2. Numerical model of a guiderail of the SP-05/2 system: a) guiderail composed of segments connected by beam elements representing screw joints; b) guiderail as a continuous beam**

## 5. TB11 virtual crash tests

The results of simulations of the TB11\_S and TB11\_C crash tests are shown in Fig. 3. Vehicle damage and deformation only concern the front wheelset. For a barrier composed of 4 m segments, the vehicle is close to non-compliance with the standard condition concerning exit in the reflectance field (Fig. 4). The vehicle and barrier interaction length is 8.90 m. During the collision, damage (erosion) of beam elements reflecting the work of guiderail screw joints does not occur. In case of a continuous guiderail, smooth repulse of the vehicle occurs in the standard reflectance field (Fig. 5). The vehicle and barrier interaction length is 8.31 m.

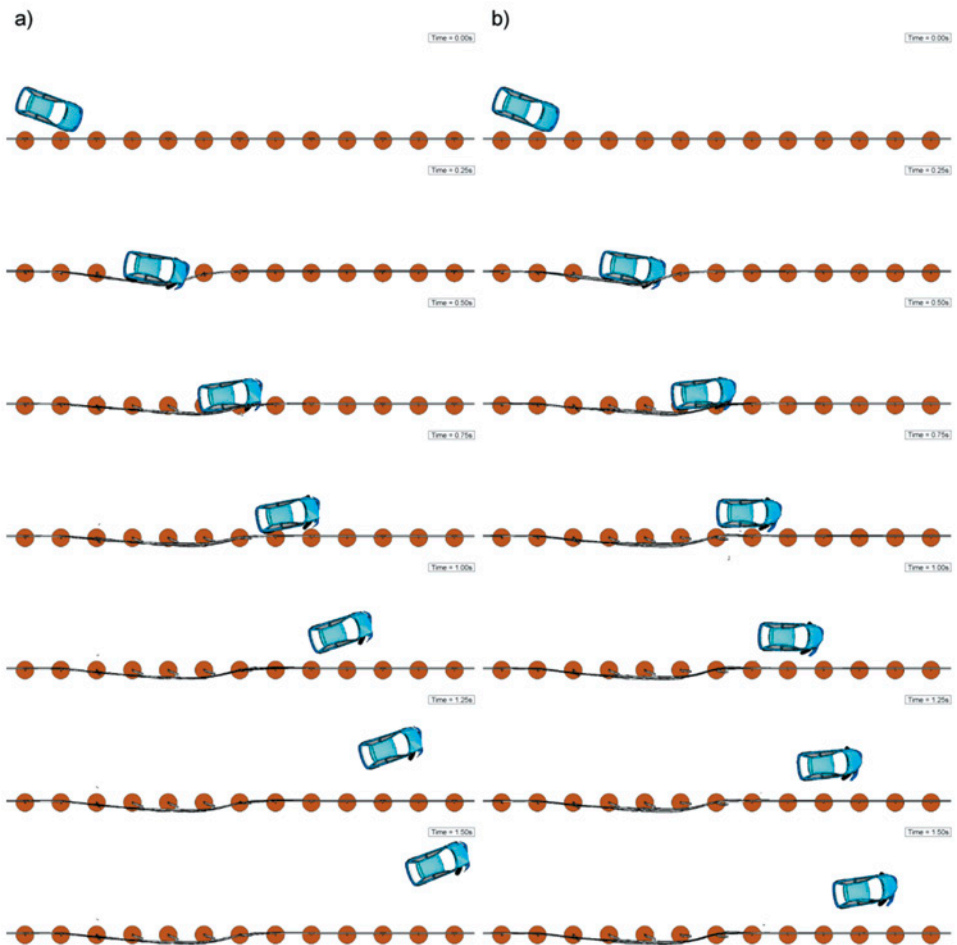
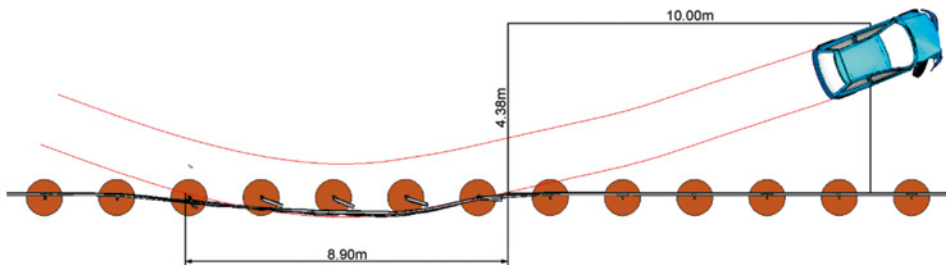


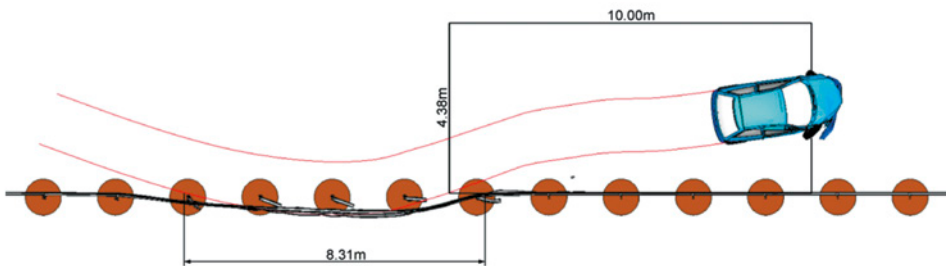
Fig. 3. Animation of the TB11 crash test – top view: a) TB11\_S; b) TB11\_C

Fig. 6 shows a comparison of energy balance of both tests. For the TB11\_S test, 85.1 % of the kinetic energy of the vehicle is absorbed as a result of the collision, and the amount of energy absorbed due to damage of materials is 0.168 MJ. The residual velocity of the vehicle at the moment of ending of the vehicle and barrier interaction ( $t = 0.716$  s) is 47.2 km/h. For the TB11\_C test, 92.5 % of the kinetic energy of the vehicle is absorbed as a result of the collision, and the amount of energy absorbed due to damage of materials is 0.189 MJ. The residual velocity of the vehicle at the moment of ending of the vehicle and barrier interaction ( $t = 0.644$  s) is 36.7 km/h.

Table 1 shows a comparison of results of the performed TB11 virtual crash tests. In comparison with a guiderail composed of 4 m segments, use of a guiderail in the form of a continuous beam caused the ASI to increase by 3.7 % as well as the THIV to decrease by 1.7 %, the working width by 2.3 %, the vehicle and barrier interaction length by 6.6 %, and the residual velocity by 22.2 %.



**Fig. 4. Vehicle exit after a collision with a barrier and the vehicle and barrier interaction length for the TB11\_S crash test – top view**



**Fig. 5. Vehicle exit after a collision with a barrier and the vehicle and barrier interaction length for the TB11\_C crash test – top view**

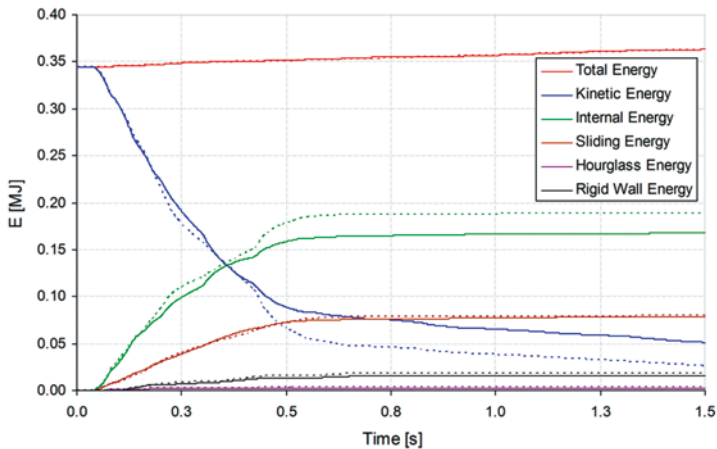


Fig. 6. Comparison of energy balance of the TB11 tests: TB11\_S – solid lines; TB11\_C – dashed lines

## 6. TB32 virtual crash tests

The results of simulations of the TB32\_S and TB32\_C crash tests are shown in Fig. 7. Vehicle damage and deformation only concern the front wheelset. For a barrier composed of 4 m segments, the vehicle has proper exit in the standard reflectance field (Fig. 8). The vehicle and barrier interaction length is 18.44 m. For a continuous guiderail, vehicle exit in the standard reflectance field is proper as well (Fig. 9). The vehicle and barrier interaction length is 17.64 m.

Fig. 10 shows a comparison of energy balance of both tests. For the TB32\_S test, 61.2 % of the kinetic energy of the vehicle is absorbed as a result of the collision, and the amount of energy absorbed due to damage of materials is 0.346 MJ. The residual velocity of the vehicle at the moment of ending of the vehicle and barrier interaction ( $t = 1.012$  s) is 62.8 km/h. For the TB32\_C test, 69.9 % of the kinetic energy of the vehicle is absorbed as a result of the collision, and the amount of energy absorbed due to damage of materials is 0.364 MJ. The residual velocity of the vehicle at the moment of ending of the vehicle and barrier interaction ( $t = 1.044$  s) is 57.6 km/h.

Table 1 shows a comparison of results of the performed TB32 virtual crash tests. In comparison with a guiderail composed of 4 m segments, use of a guiderail in the form of a continuous beam caused the ASI to decrease by 7.4 %, the THIV by 6.8 %, the working width by 9.3 %, the vehicle and barrier interaction length by 4.3 %, and the residual velocity by 8.1 %.

During a car and barrier collision in the TB32 tests, erosion (damage) of two beam elements reflecting the performance of guiderail segment screw joints occurs (fig. 11). Nevertheless, the guiderail continuity is preserved.



Fig. 7. Animation of the TB32 crash test – top view: a) TB32\_S; b) TB32\_C

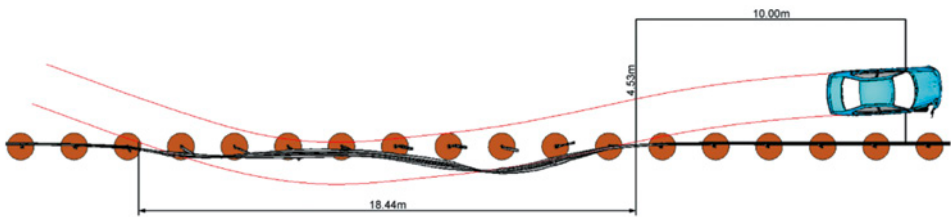


Fig. 8. Vehicle exit after collision with a barrier and the vehicle and barrier interaction length for the TB32\_S crash test – top view

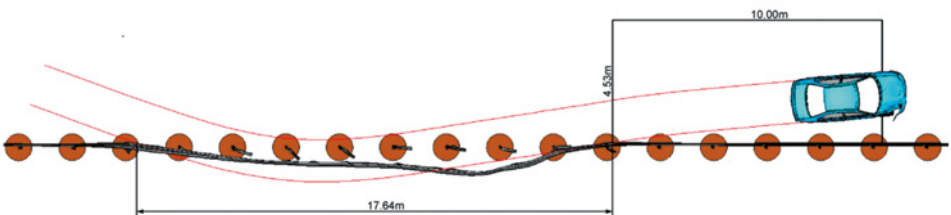


Fig. 9. Vehicle exit after a collision with a barrier and the vehicle and barrier interaction length for the TB32\_C crash test – top view

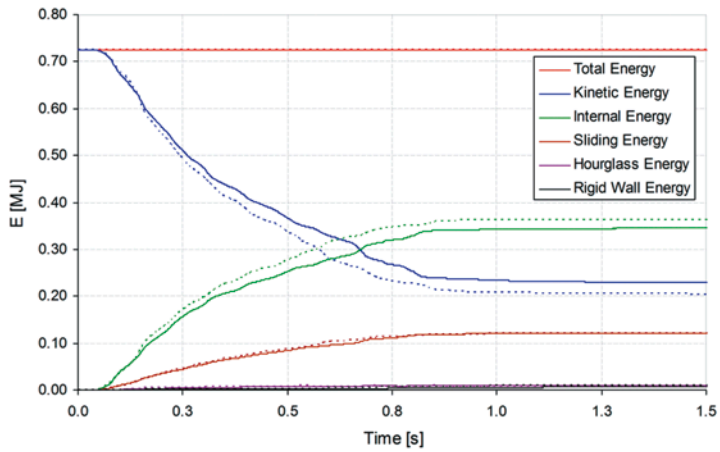


Fig. 10. Comparison of energy balance for the TB32 tests: TB32\_S – solid lines; TB32\_C – dashed lines

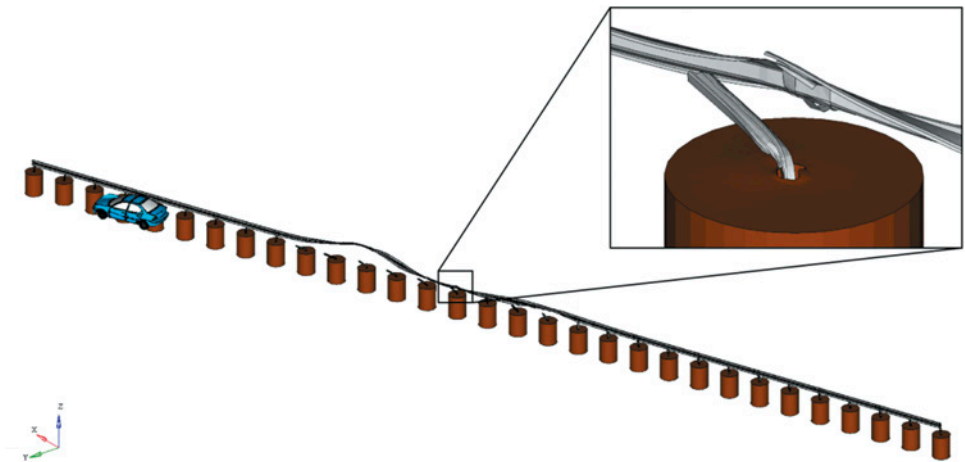


Fig. 11. Damage of two bottom screw joints of a guideway

**Table 1. Comparison of the results of the analysed virtual crash tests**

<b>Dynamical system</b>	<b>ASI</b>	<b>THIV [km/h]</b>	<b>VCDI</b>	<b>Wm [m]</b>	<b>L<sup>1)</sup> [m]</b>	<b>PPQ<sup>2)</sup></b>	<b>E<sup>3)</sup> [MJ]</b>	<b>vr<sup>4)</sup> [km/h]</b>
Experiment [17]	0.8	23	RF0001000	1.1	-	-	-	-
TB11_S	0.78	20.23	RF0010000	0.87	8.90	yes	0.168	47.2
TB11_C	0.81	19.89	RF0010000	0.85	8.31	yes	0.189	36.7
TB32_S	0.68	17.99	RF0010000	1.29	18.44	yes	0.346	62.82
TB32_C	0.63	16.76	RF0010000	1.17	17.64	yes	0.364	57.62

<sup>1)</sup> length of the vehicle/barrier interaction section

<sup>2)</sup> proper behaviour of the car in the reflectance field

<sup>3)</sup> energy absorbed due to damage of materials

<sup>4)</sup> residual velocity at the moment of vehicle exit from the interaction with the barrier

## 7. Recapitulation

The work presented the effect of the B-type guiderail joints of a SP-05/2 barrier on the course of the TB11 and TB32 virtual crash tests. The guiderail was modelled as a continuous beam (without joints) and as a system composed of 4 m long segments connected with beam elements reflecting screw joints. In case of the TB11 test, assumption of the guiderail as a continuous beam causes correct vehicle repulse by the barrier. Taking of screw joints of guiderail segments into account causes the criterion of vehicle exit to be close to non-compliance. For the TB32 test, this effect does not occur. For both tests, TB11 and TB32, there is a decrease of crash parameters in case of a guiderail modelled as a continuous beam (except the ASI parameter for the TB11 test). Taking of guiderail segment joints into account is of crucial importance in case of numeric tests of new restraint systems. In such condition, it is possible to check whether the system maintains its continuity and integrity during a collision (the guiderail is not broken) or whether the vehicle is properly repulsed to the carriageway.

## Acknowledgements

The study has been performed under the PBS1/B6/14/2012 research project (acronym: ENERBAR), financed in 2013–2015 by the National Centre of Research and Development.

The full text of the Article is available in Polish online on the website <http://archiwummotoryzacji.pl>.

Tekst artykułu w polskiej wersji językowej dostępny jest na stronie <http://archiwummotoryzacji.pl>.

## References

- [1] Atahan A O. Finite element simulation of a strong-post W-beam guardrail system. *Simulation*. 2002; 78(10): 587-599.
- [2] Borovinssek M, Vesenjsek M, Ulbin M, Ren Z. Simulation of crash test for high containment levels of road safety barriers. *Engineering Failure Analysis*. 2007; 14(8): 1711-1718.
- [3] Dziejwski P. Numerical analysis of car – road barrier crash tests. *Proc. III Symp. on Advances in Manufacturing Technologies and Machinery Structures*; 2009; Kazimierz Dolny, Poland.
- [4] Engstrand K E. Improvements to the weak-post W-beam guardrail [master thesis]. Worcester Polytechnic Institute; 2000. 130 p.
- [5] Goubel C, Di Pasquale E, Massenzio M, Ronel S. Comparison of crash tests and simulations for various vehicle restraint systems. 7th European LS-DYNA Conference. DYNAMore, GmbH; 2009; Detroit, USA.
- [6] Hallquist J O. LS-DYNA Keyword User's Manual. Livermore Software Technology Corporation. 2007.
- [7] Hallquist J O. LS-DYNA Theory Manual. Livermore Software Technology Corporation. 2006.
- [8] Klasztorny M, Kiczko A, Nycz D. Modelowanie numeryczne i symulacja rozciągania połączenia śrubowego segmentów prowadnicy B bariery drogowej. *Konferencja Naukowo-Techniczna Techniki Komputerowe w Inżynierii*; 2014; Licheń Stary, Polska, 77-78.
- [9] Klasztorny M, Nycz D, Romanowski R K. Rubber/foam/composite overlay onto guide B of barrier located on road bend. *The Archives of Automotive Engineering – Archiwum Motoryzacji*. 2016; 69(3): 65-86.
- [10] Klasztorny M, Romanowski R K, Nycz D. Nakładka kompozytowo-pianowa na prowadnicę B drogowej bariery ochronnej w łuku poziomym wklęsłym – część 2: Modelowanie i symulacja testów zderzeniowych. *Materiały kompozytowe*. 2015; 4: 8-10.
- [11] Nycz D. Modelowanie i badania numeryczne testów zderzeniowych bariery klasy N2-W4-A na łukach dróg [dissertation]. *Wojskowa Akademia Techniczna*; 2015.
- [12] Ren Z, Vasenjsek M. Computational and experimental crash analysis of the road safety barrier. *Engineering Failure Analysis*. 2005; 12(6): 963-973.
- [13] Vasenjsek M, Borowinssek M, Ren Z. Computational simulations of road safety barriers using LS-DYNA. *LS-DYNA Anwenderforum, Frankenthal*; 2007: 1-8.
- [14] PN-EN 1317-1:2010. Systemy ograniczające drogę – część 1: Terminologia i ogólne kryteria metod badań.
- [15] PN-EN 1317-2:2010. Systemy ograniczające drogę – część 2: Klasy działania, kryteria przyjęcia badań zderzeniowych i metody badań barier ochronnych i balustrad.
- [16] *Stalowe bariery ochronne*. Stalprodukt S.A.; 2006, Bochnia.
- [17] *System N2 W4 (SP-5/2)*. Stalprodukt S.A.; 2011, Bochnia.
- [18] *Vehicle Models* (cited 18 Sep 2014). Available from: <http://www.nacac.gwu.edu/vml/models.html>.
- [19] *The American Association of State Highway and Transportation Officials. Manual for Assessing Safety Hardware* (cited 18 Sep 2014). Available from: [http://books.google.pl/books?id=LV0mSYE9-SOC&printsec=frontcover&hl=pl&source=gbs\\_ge\\_summary\\_r&cad=0#v=onepage&q&f=false](http://books.google.pl/books?id=LV0mSYE9-SOC&printsec=frontcover&hl=pl&source=gbs_ge_summary_r&cad=0#v=onepage&q&f=false).

